Compatibility of TPD/Polycarbonate Blends by ^{13}C–^{1}H HETCOR in the Solid State

S. Kaplan

Xerox Webster Research Center, 800 Phillips Road 0114-39D, Webster, New York 14580

Received June 5, 1992; Revised Manuscript Received November 20, 1992

ABSTRACT: Two-dimensional heteronuclear ^{13}C–^{1}H NMR measurements in the solid state have been used to investigate the compatibility of a solvent cast blend of an aromatic diamine, *N,N'*-diphenyl-*N,N'*-bis(3-methylphenyl)-1,1'-biphenyl-4,4'-diamine (TPD) in Bisphenol A polycarbonate. Measurements of carbon–proton correlations as a function of proton spin diffusion time, inserted between the proton evolution and cross-polarization periods, are interpreted in terms of an initial fast response from both inter- and intramolecular dipolar couplings and a slower response only from intermolecular couplings. The 2-D technique is capable of observing spin diffusion between domains even though there are no resolved peaks from the individual components in the ^{1}H dimension. Distinction between domains is based upon the differences in aliphatic and aromatic proton populations of the individual components or on differences in proton projection line shapes for unique carbon resonances from each component. From these results it is shown that, although there is a distribution of separations of the small molecule amine from the polymer binder, inter- and intramolecular spin diffusion occur at similar rates, indicative of intimate mixing at the molecular level.

Introduction

Useful properties of polymers can be obtained by blending with other polymers or small molecules.[1] Control over these properties often can be achieved by modifying the domain morphology of the composite material. A number of techniques, including thermal analysis, dielectric and dynamic mechanical spectroscopy, electron microscopy, and neutron scattering have been applied to the problem of characterizing morphology of polymeric systems. One drawback of these methods is that they cannot directly identify the individual structures in distinct regions of a multicomponent system. Using nuclear magnetic resonance, on the other hand, not only are local nuclear interactions (e.g., dipole–dipole, chemical shift) able to distinguish fine structural differences that elude these other measurements but longer range mechanisms (e.g., spin diffusion) allow for characterizing molecular homogeneity on a scale of up to a few hundred angstroms.

Solid-state NMR techniques have been used to characterize domain structure in polymeric systems. These experiments are based upon the classic Goldman–Shen experiment,[2] in which the time for spin diffusion to transfer magnetization order from one domain to another is used to measure domain size. The overriding consideration in determining the applicability of the Goldman–Shen method is the ability to resolve individual components so that an initial magnetization gradient between domains can be created. In the original method, domains are distinguished by proton line width differences, which can originate from differences in either spin densities[3,4] or motional correlation times.[5–10] In cases where dipolar line width differences are insufficient, multiple pulse abundant spin line narrowing sequences have been applied to distinguish the components using dipolar (based on linewidths)[11] or chemical shift[4,12,13] filters. A natural extension of these experiments is to utilize the Goldman–Shen experiment as a proton preparatory sequence, followed by cross polarization with ^{13}C nuclei for subsequent high-resolution carbon detection. Such techniques have been performed by employing either proton dipolar filters[4,10,14] or proton chemical shift filters[15] to create an initial magnetization gradient. High-resolution detection afforded by these experiments permits assignment of the chemical constituents between which spin diffusion takes place. The higher resolution relative to proton observation, however, is obtained at the expense of lower sensitivity.

The above mentioned techniques require that resolution of proton resonances in the separate domains, whether it be via line width or chemical shift, be achievable. It is, however, possible to relax this restriction somewhat in the multipulse proton detection experiment by judicious choice of the initial preparatory condition, if the proton line shapes of the individual components differ significantly.[16] Alternatively, one can utilize a two-dimensional ^{13}C–^{1}H heteronuclear variant of these experiments, and this latter method is applied to the present problem. A number of pulse sequences have been proposed to give two-dimensional heteronuclear solid-state spectra.[17–20] Common to most of these experiments are the suppression of homo- and heteronuclear interactions during the evolution (t_1) period, transfer of magnetization to carbons from directly bonded protons while effectively suppressing proton homonuclear interactions, and ^{13}C detection (t_2 period) with ^{1}H heteronuclear decoupling. During the evolution period homonuclear dipolar couplings can be suppressed by MREV-8[17,20] or BLEW-12[18,21] windowless multiple pulse sequences, and these may be applied concurrently with continuous irradiation[17] or WALTZ-8[18] saturation of rare spins for heteronuclear dipolar coupling suppression. More recently, Burum and Bielecki[19] have proposed combining BLEW-24 and BB-24 sequences as a more effective means of simultaneously reducing homo- and heteronuclear interactions during the proton evolution period. They also utilized WIM-24[18] for isotropic coherence transfer from protons to carbons.[18] Their method has been applied to investigate the solid-state structure of amorphous poly(2,6-dimethyl-*p*-phenylene oxide) (PPO).[22] In that study, correlation peaks in the 2-D spectrum were used to measure conformations of adjacent rings in the polymer backbone.

This technique can probe distances of up to a few angstroms. However, by addition of a mixing period for ^{1}H spin diffusion after the evolution period, measurement can be extended to longer range ^{1}H–^{1}H interactions.[20] Such experiments have been carried out recently to analyze the conformation of poly(2,5-dimethoxy-*p*-phenylenevinylene) (PDMPV).[23] From spin diffusion rates, measured by coherence transfer from one crosspeak to another, average distances between the methoxy, aromatic, and vinylene

0024-9297/93/2226-1060$04.00/0

protons were measured and used to calculate dihedral angles. The ability to probe intermolecular distances is enabling also the study of polymer blend compatibility, the subject of the present study.

The system under investigation of this work is a blend of an aromatic diamine, *N,N'*-diphenyl-*N,N'*-bis(3-methylphenyl)-1,1'-biphenyl-4,4'-diamine (TPD) in Bisphenol A polycarbonate. Interest in this blend stems from its use as a charge transport layer in photoconductors. These blends form excellent electronic hole transporting layers,[24,25] and homogeneous blending is presumed essential to achieving high transport rates. Pure TPD is highly crystalline, with a melting point of T_m = 167 °C and a glass transition temperature of T_g = 63 °C.[26] A well-mixed 50/50 (wt/wt) blend with polycarbonate (T_g = 137 °C) cast from methylene chloride is amorphous and shows a single T_g of ~89 °C. Partial phase separation of the blend can be induced by heating to temperatures close to that of the T_g of polycarbonate or by inducing stress. Differential scanning calorimetry (DSC) measurements suggest that phase separation is the result of crystallization of TPD by nucleation around trapped impurities.[26]

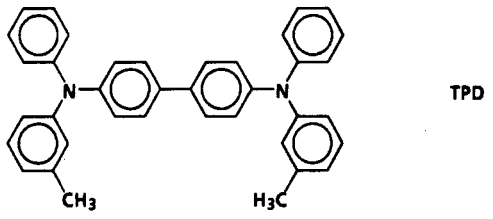

TPD

Proton spin–lattice and spin–spin relaxation studies have been performed on this system.[27] These studies show results similar to those of DSC measurements in that a well-prepared blend has a single relaxation behavior, whereas multiple domains can be observed from samples treated with appropriate thermal or stress history. Our goal here is to ascertain the degree of mixing of a blend cast from methylene chloride, which is the solvent used for the preparation of photoreceptor transport layers.

Experimental Section

Material Preparation. *N,N'*-diphenyl-*N,N'*-bis(3-methylphenyl)-1,1'-biphenyl-4,4'-diamine (TPD) was synthesized by the procedure described earlier.[24] The purified material is a crystalline powder. Blends with polycarbonate were prepared by casting films from methylene chloride. An 8-mm-wide strip of approximately 100 mg of the 50/50 film was rolled into the shape of a cylinder for insertion into the rotor used for magic angle spinning NMR spectroscopy.

NMR Spectroscopy. All solid-state NMR spectra were obtained on a Bruker CXP spectrometer operating at 200 MHz for ^{1}H in a Cryomagnet Systems, Inc. 47 kG wide-bore superconducting magnet system. ^{13}C cross-polarization measurements at 50.3 MHz used 3-ms mixing times, high-power (H_1 = 50 kHz) ^{1}H decoupling, and a recycle time of 2.5 s. Magic angle spinning at 3.6–4.0 kHz was performed in a Doty Scientific probe with 100 mg of sample packed into 6-mm sapphire rotors. A one-time angle adjustment was accomplished by maximizing the spinning sideband intensities of a sample of KBr. Spectra are referenced to tetramethylsilane by assigning the methyl peak of a separately run sample of hexamethylbenzene to 17.36 ppm.

Heteronuclear two-dimensional spectroscopy (Figure 1) employed ^{1}H and ^{13}C $\pi/2$ pulses of 3.7 μs and 512 scans per spectrum. The proton evolution period consisted of 0–50 BLEW-24 cycles of 88.8 μs (24 × 3.7 μs), which defines the dwell time in the F1 (proton) dimension. Simultaneously, BB-24 is applied to carbons in order to suppress heteronuclear dipolar interactions with protons. After the evolution period, a 63° pulse (orthogonal to the initial $\pi/2$ preparation pulse) is applied to tilt the proton magnetization into the xy plane, subsequently followed by a $\pi/2$ selection pulse that cycles sequentially (for each value of t_1) through all four rf phases to enable TPPI acquisition in the proton (F1) dimension. Isotropic cross polarization was achieved using one cycle (88.8 μs) of WIM-24 on both carbons and protons, and finally ^{13}C data were acquired with proton decoupling. In all experiments the TOSS sequence[28] is applied to the carbon spins for suppression of spinning sidebands.

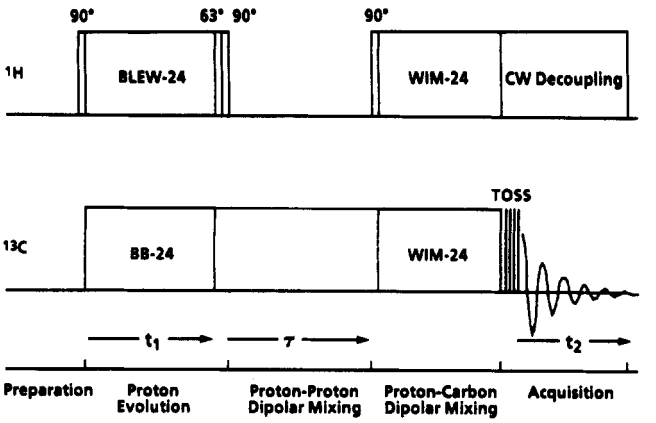

Figure 1. Pulse sequence for achieving heteronuclear correlated spectra with spin diffusion in the solid state. For the experiment without spin diffusion, the dipolar diffusion period and the subsequent 90° pulse are omitted.

For spin diffusion measurements a $\pi/2$ selection pulse, which sequentially (for each value of t_1) nutates each of the four rf phases (for TPPI acquisition) to the z direction, followed by an adjustable waiting period (1–2000 μs) with carbon decoupling, is inserted after the tilt pulse. During this time, proton–proton spin diffusion occurs so that the subsequently cross-polarized carbon signal reflects carbon–proton interactions over extended distances. In order to avoid artifacts near zero frequency in the proton dimension, an offset of −1000 Hz from resonance is implemented during all but the acquisition period of the experiment. The proton chemical shift scaling factor was determined experimentally to be ~0.43 by varying the proton offset frequency. Short proton T_1 values for polycarbonate and the compatible blend permitted experiment recycle times of 2.5 s. However, for the physical mixture, long T_1 values of 10–15 s for the pure TPD component necessitated 60-s recycle times.

Processing of two-dimensional data was performed on a Sun SparcStation using the Felix software package written by Hare Research, Inc.

Results and Discussion

Figure 2a shows the cross-polarization ^{13}C spectrum with magic angle spinning of pure TPD. This material is crystalline and the X-ray structure indicates four molecules per unit cell,[29] thus explaining the splittings of a number of the resonances. When blended 50/50 (wt/wt) with polycarbonate, the spectrum, shown in Figure 2b, shows partial resolution of TPD and polycarbonate. Resolved TPD splittings are absent from the spectrum of the blend, since the blend is completely amorphous.

The two-dimensional heteronuclear spectrum of TPD in polycarbonate is shown in Figure 3. Because proton–proton couplings are suppressed by the BLEW-24 pulse train during the proton evolution period, correlated peaks reflect primarily short-range directly bonded proton–carbon correlations. Severe overlap in the aromatic region permits unique assignment of only one contour to a single component—the 140 ppm ^{13}C resonance attributed to C9 of TPD. On the other hand, all three contours in the aliphatic region can be uniquely assigned. Most diffusion (e.g., Goldman–Shen and its variants) experiments are not useful for this sample, since the ^{1}H spectrum cannot resolve distinct peaks from the two components. However, the HETCOR experiment is applicable and, as is shown below, enables estimation of internuclear distances.

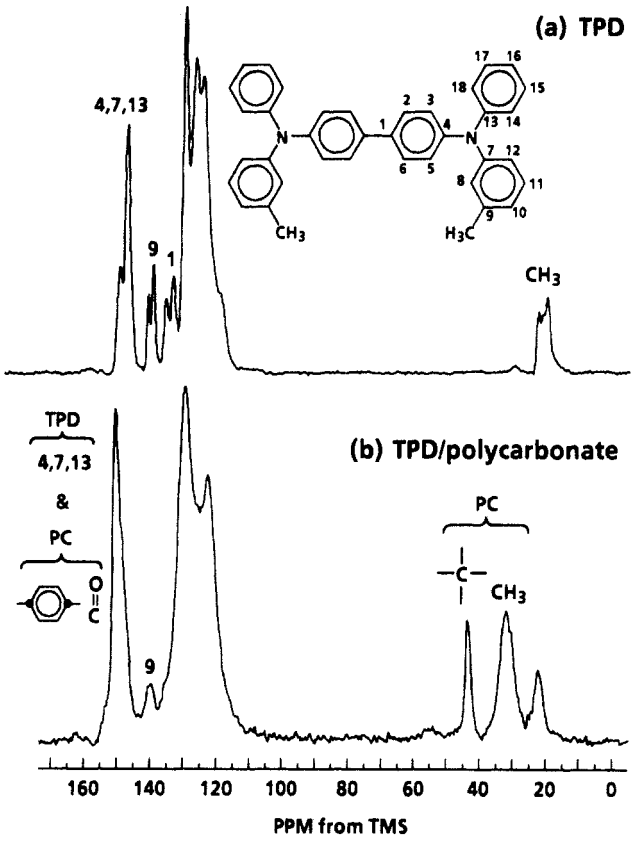

Figure 2. (a) Cross polarization ^{13}C spectrum with 5-kHz magic angle spinning (CPMAS) of pure TPD. The TOSS sequence was used to suppress spinning side bands. (b) CPMAS spectrum of TPD blended with polycarbonate (50/50 wt/wt).

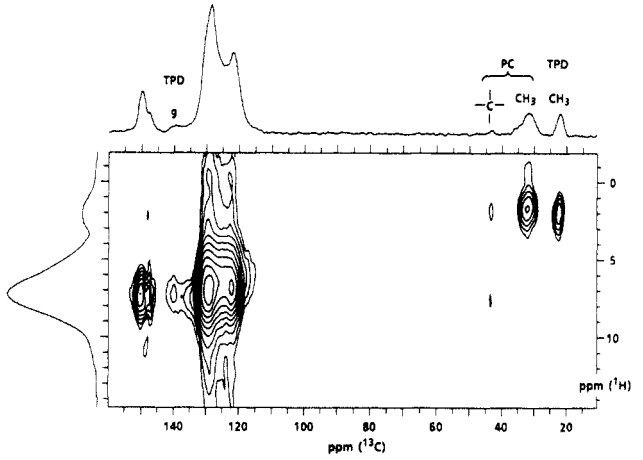

Figure 3. Two-dimensional HETCOR spectroscopy of TPD in polycarbonate (50/50 wt/wt) acquired with the pulse sequence of Figure 1, but without a spin diffusion period.

Proton–proton dipolar exchange mixing can be monitored by varying the spin diffusion time in the experiment of Figure 1. The ^{13}C aliphatic region of the spin diffusion contour maps for the 50/50 blend as a function of diffusion time is shown in Figure 4. For short times the aliphatic peak correlations primarily reflect directly bonded or, in the case of the quaternary carbon, nearest neighbor carbon–proton interactions. After only 20 μs (Figure 4a) of mixing, the two-dimensional spectrum is nearly identical to the spectrum without a spin diffusion mixing period (Figure 3). However, with increasing mixing times (Figure 4b–d), the correlation between the methyl carbons and aromatic protons intensifies. This trend occurs because longer range interactions come into play as spin diffusion transfers magnetization from the aromatic protons to the

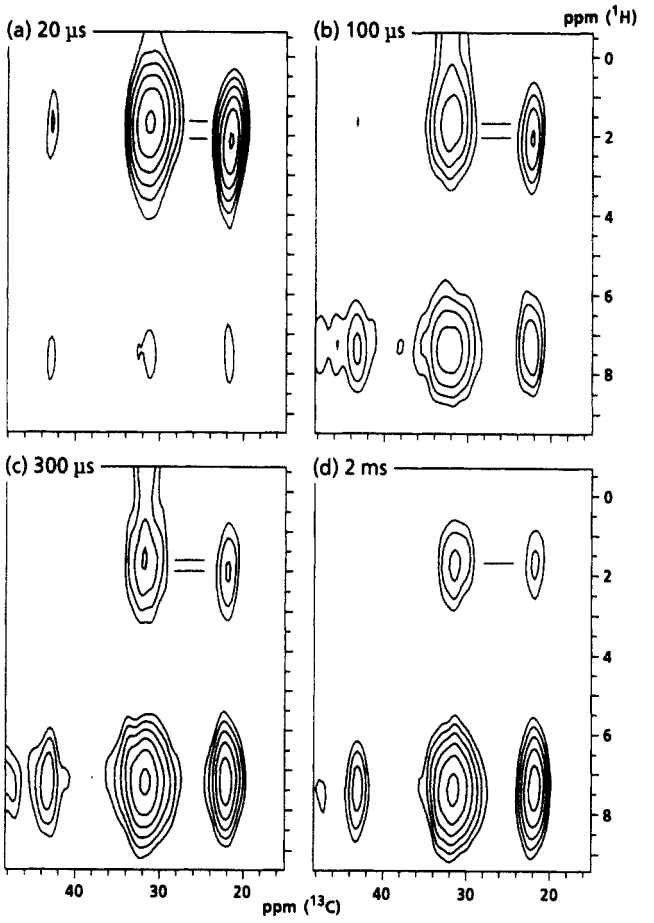

Figure 4. Aliphatic region of the HETCOR spectra of the TPD/polycarbonate blend as a function of dipolar spin diffusion time in the experiment of Figure 1. Spectra along both the ^1H and ^{13}C axes are referenced to TMS at δ = 0 ppm.

methyl protons, which isotropically cross polarize with the methyl carbons during the WIM-24 pulsing. Ultimately, for long spin diffusion times, the relative signal intensities for the contours associated with a particular carbon will reflect quantitatively the chemical shift distribution of protons that are within an effective range of spin diffusion from the protons directly bonded to that carbon. During the proton evolution time (t_1) the magnetization of each proton evolves according to its unique chemical shift, which modulates the ^{13}C chemical shifts via WIM-24 cross polarization. For long spin diffusion times, all protons eventually come to a common spin temperature, thereby encoding into the magnetization of each proton equally weighted chemical shift information from all protons in the sample. Thus, the carbon signal that develops from subsequent cross polarization is modulated as a function of t_1 by the superposition of chemical shifts from all of the protons. Data in the recent publication by Simpson et al.[23] (refer to their Figure 5a) can be used to illustrate this point. HETCOR measurements on *p*-dimethoxybenzene for long spin diffusion times show relative proton intensities for the methoxy carbon correlations of 6:2:2 for the methoxy:downfield aromatic: upfield aromatic protons, corresponding to their relative populations in the molecule.

Figure 5 shows plots of the volume integral fraction of aliphatic protons, $V_{aliphatic}/(V_{aliphatic} + V_{aromatic})$, for the polycarbonate (open symbols) and TPD (closed symbols) methyl carbons as a function of spin diffusion time, τ. Both curves asymptote to an aliphatic volume fraction of 0.3, which corresponds exactly to the fraction of protons in the entire sample that are from methyl groups. Thus,

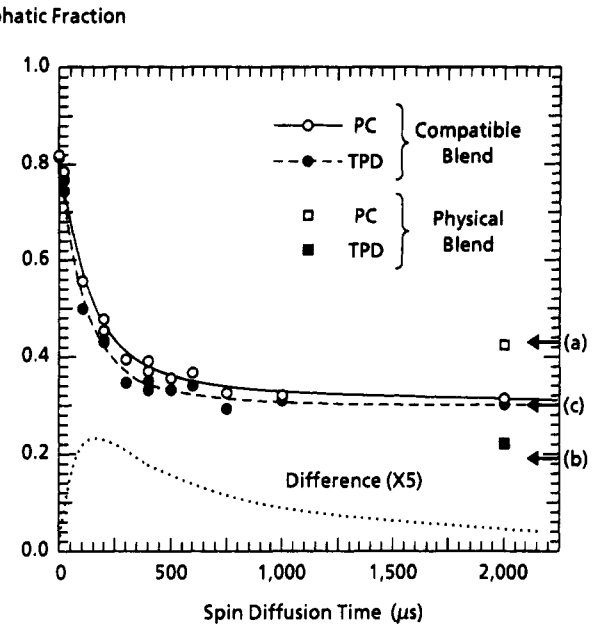

Figure 5. Evolution of the aliphatic proton correlations for the TPD (closed circles) and polycarbonate (open circles) methyl carbons as a function of spin diffusion mixing time, τ, for the 50/50 compatible blend. Double exponential nonlinear regression fits are shown for visualization and to compute the difference response (scaled by a factor of 5). Shown for comparison are long-term diffusion results for a physical blend of the same composition.

within ~1 ms nearly all of the protons of the system achieve a common spin temperature via spin diffusion. Also shown on this plot are the results of a diffusion time of τ = 2 ms for the polycarbonate and TPD methyl carbons in a simple (50/50 wt/wt) physical blend of the two solids. For the very large domains present in the physical blend, spin diffusion during 2 ms can only occur intramolecularly. Therefore, the expected volume fraction of the aliphatic proton contour for the polycarbonate methyl carbon resonance should be 0.429 (point a in Figure 5), i.e., the aliphatic proton fraction in polycarbonate. The corresponding value for TPD is 0.188 (point b). The actual measured values are quite close to these predictions. Both curves for the compatible blend have been fit by double exponentials. At the bottom of Figure 5 is plotted their difference, which can be interpreted in terms of a fast initial rise from both inter- and intramolecular and a slower long-term decay from intermolecular proton spin diffusion. The driving force for the initial rise is the lower aliphatic proton fraction in TPD than in polycarbonate. It is important to note that fitting the data to exponentials is not meant to imply any mechanism for spin diffusion but does suggest the two-component response of the diffusion behavior.

Inter- and intramolecular processes cannot be fully separated, since there is a substantial amount of intermolecular spin diffusion occurring at the rate of the intramolecular process. If all of the intermolecular processes occurred at the slower rate, the extrapolated intercept for the slower component would be at (a) − (b) or 0.24, which is 4 times larger than actually observed. Therefore, there must be a distribution of intermolecular distances, with the shortest being on the order of intramolecular distances. The time constant for the initial rise in Figure 5 is reasonable in view of the time constant of less than 100 μs observed in a homopolymer of poly (2,5-dimethoxy-*p*-phenylenevinylene) (PDMPV).[23] Because proton spin densities for PDMPV and polycarbonate are similar, it is expected that polycarbonate homopolymer

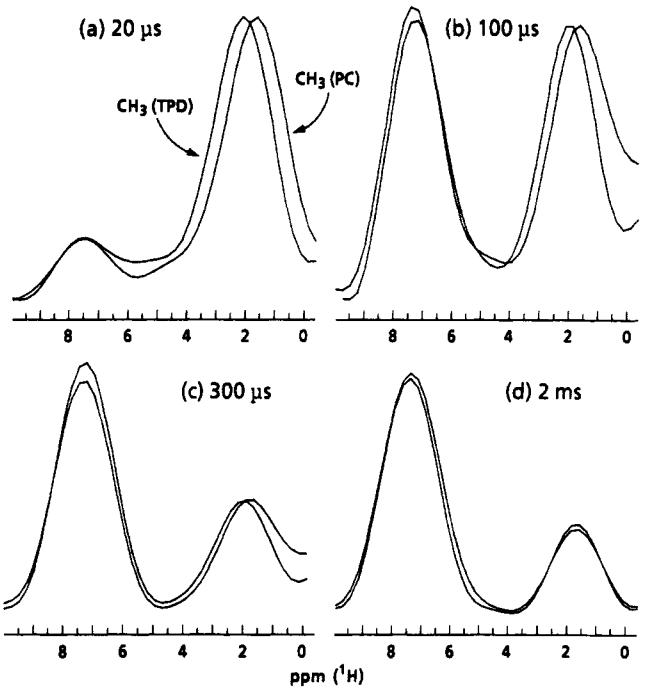

Figure 6. Projections along the ^{1}H axis of the contour plots in Figure 4 as a function of mixing time τ.

will exhibit similar intramolecular spin diffusion times.

An alternate treatment of the data in Figure 4 can be used to obtain the rate of intermolecular diffusion. In Figure 6 are superimposed plots of the proton slices (more precisely, the sum of slices over the carbon full width at half-maximum) through the methyl carbon resonances at 33 ppm for polycarbonate and 22 ppm for TPD. With increasing spin diffusion time, the aromatic proton signal intensities increase, as discussed previously and shown in Figure 5. Since the only upfield peaks in the proton spectra of both polycarbonate and TPD are from methyl groups, changes in the shape of the aliphatic regions of Figure 6 can only result from dipolar diffusion from the methyl protons of one component to the methyl protons of the other. These line shapes become increasingly similar as spin diffusion transports polarization between TPD and polycarbonate. In order to represent this progression graphically, we have evaluated the correlation, i.e., the mean square difference for each pair of methyl proton signals. This calculation is performed within the half-height width of the proton peaks, and integrals for each pair of peaks are first normalized to the same value. The mean square deviations thus calculated are normalized to 1 for short mixing times and plotted in Figure 7 as a function of $\tau^{1/2}$. Although there is considerable scatter, the data extrapolate to 0 (i.e., methyl peaks are superimposable) for $t \sim 1$ ms. Similarly, a plot (not shown) of proton peak separation vs $\tau^{1/2}$ yields 1 ms for the extrapolated time for positional overlap. The diffusive path length, r, which represents half of the smallest domain dimension, can be estimated[9,16,30] from $r = (nD\tau)^{1/2}$, where n is depends upon the domain shape and is $^4/_3$ for lamellar morphology,[11] τ is the the spin diffusion time, and D is the spin diffusion constant, typically 5×10^{-12} cm^2 s^{-1}. The approximate time of 1 ms for spin diffusion to occur between methyl groups corresponds to domains with a smallest dimension of ~1.6 nm. This value is on the order of the repeat unit dimension in polycarbonate, supporting the conclusion that intimate mixing occurs in the blend.

Studies of hole transport show a strong impact of the binder polymer on hole mobility.[31] It has been suggested that higher hole mobility of TPD in polystyrene vs TPD

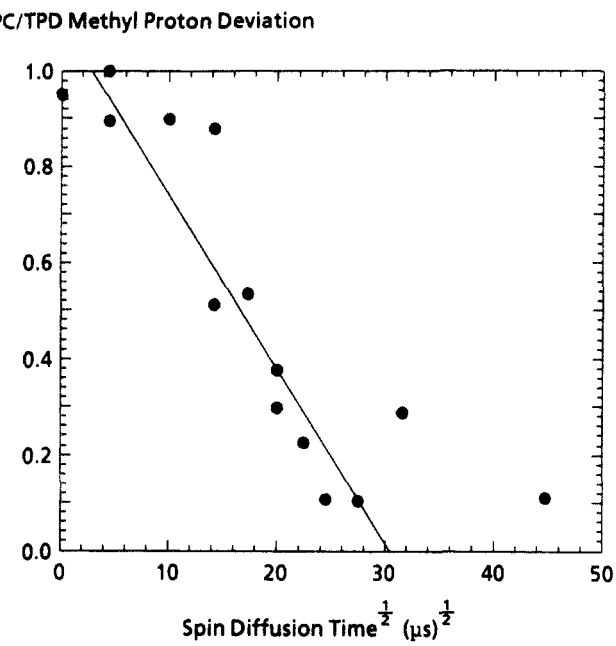

Figure 7. Normalized mean square deviation of the polycarbonate and TPD methyl group proton projections in Figure 6 as a function of (spin diffusion time)$^{1/2}$. Data represent the mean squared differences for each pair of signals in the aliphatic region of the plots in Figure 6.

in polycarbonate can be explained by the effect of dipole–dipole interactions between polymer chains on the alignment of TPD molecules and hence on the wave function overlap, which is required for transport. This argument would require compatibility at the molecular dimensions found in the current work. Evidence from calorimetric measurements of the polycarbonate/TPD blends[26] demonstrates that phase separation can be induced by heating the sample to just below the polycarbonate T_g, provided that there are crystallization impurity sites available. A sample prepared by heating to 110 °C overnight became visibly opaque. HETCOR diffusion spectra of this sample were obtained, but there was negligible difference from the data of the clear films. Thus it would appear that only a small fraction of material (e.g., surface only) has thermally phase separated. Although T_1 of highly crystalline pure TPD is long (~10–15 s), the same short delays were used for HETCOR measurements of the heated material as for the well-mixed blend. Longer delays were not necessary, since the polycarbonate carbon response in the 2-D experiment as a function of spin diffusion time should be sensitive to phase separation, either by virtue of increased intermolecular distances or from the lack of TPD proton response resulting from long T_1 values.

In summary, incorporation of a spin diffusion time into the two-dimensional heteronuclear correlated pulse sequence enables measurement of longer range proton–proton dipolar couplings in the solid state. We have demonstrated the ability of the technique to probe internuclear separations in blends of TPD and polycarbonate, even though there is insufficient chemical shift resolution along the proton dimension to resolve the two components. It also should be possible to approach this problem with a multiple pulse proton observe sequence by optimizing the chemical shift based polarization gradients,[16] since there is, in fact, a sizable difference in the aromatic:aliphatic signal ratios for the individual components of the blend. The present method, however, does offer the intuitive appeal of being able to resolve individual component carbon chemical shifts. As with the Goldman–Shen experiment, the maximum domain sizes measureable by the 2-D technique are limited by proton T_1. Thus, for polymer blends, realistic expectations are that domains with linear dimensions of up to approximately 30 nm are accessible. The present data show that a methylene chloride cast blend of the aromatic amine TPD in Bisphenol A polycarbonate is compatible at the molecular level. This result is consistent with the level of compatibility found by previous NMR measurements of cross-polarization rates between domains of a similar aromatic amine, tri-*p*-tolylamine, and polycarbonate.[32]

Acknowledgment. D. Burum of Bruker Instruments and D. Rice of the University of Massachusetts are gratefully acknowledged for helpful discussions regarding the two-dimensional pulse sequences, and D. Rice is acknowledged for providing a preprint of work carried out at the University of Massachusetts using the diffusion experiment. Finally, the author wishes to thank J. Yanus for supplying the samples used for this study.

References and Notes

(1) Paul, D. R.; Newman, S. *Polymer Blends*; Academic Press: New York, 1978.
(2) Goldman, M.; Shen, L. *Phys. Rev.* **1966**, *144*, 321.
(3) An example is amorphous hydrogenated silicon: S. Kaplan, unpublished data.
(4) Vanderhart, D. L. *Makromol. Chem. Macromol. Symp.* **1990**, *34*, 125–159.
(5) Cheung, T. T. P.; Gerstein, B. C. *J. Appl. Phys.* **1981**, *52*, 5517–5528.
(6) Assink, R. A. *Macromolecules* **1978**, *11*, 1233–1237.
(7) Packer, K. J.; Pope, J. M.; Yeung, R. R.; Cudby, M. E. A. *J. Polym. Sci., Polym. Phys. Ed.* **1984**, *22*, 589–616.
(8) Lind, A. C. *Polym. Prepr., Am. Chem. Soc., Div. Polym. Chem.* **1980**, *21*, 241–242.
(9) Lind, A. C. *Polym. Prepr., Am. Chem. Soc., Div. Polym. Chem.* **1981**, *22*, 333–334.
(10) Belfiore, L. A.; Graham, H.; Veda, E.; Wang, Y. *Polym. Int.* **1992**, *28*, 81–94.
(11) Havens, J. R.; Vanderhart, D. L. *Macromolecules* **1985**, *18*, 1663–1676.
(12) Caravatti, P.; Neuenschwander, P.; Ernst, R. R. *Macromolecules* **1986**, *19*, 1889–1895.
(13) Caravatti, P.; Neuenschwander, P.; Ernst, R. R. *Macromolecules* **1985**, *18*, 119–122.
(14) Schmidt-Rohr, K.; Egger, N.; Domke, W. D.; Blümich, B.; Spiess, H. W. *Bull. Magn. Reson.* **1989**, *11*, 418.
(15) Schmidt-Rohr, K.; Clauss, J.; Blümich, B.; Spiess, H. W. *Magn. Reson. Chem.* **1990**, *28* (Spec. Issue), S3-S9.
(16) Campbell, G. C.; VanderHart, D. L. *J. Magn. Reson.* **1992**, *96*, 69–93.
(17) Roberts, J. E.; Vega, S.; Griffin, R. G. *J. Am. Chem. Soc.* **1984**, *106*, 2506–2512.
(18) Caravatti, P.; Braunschweiler, L.; Ernst, R. R. *Chem. Phys. Lett.* **1983**, *100*, 305–310.
(19) Burum, D. P.; Bielecki, A. *J. Magn. Reson.* **1991**, *94*, 645–652.
(20) Caravatti, P.; Bodenhausen, G.; Ernst, R. R. *Chem. Phys. Lett.* **1982**, *89*, 363–367.
(21) Burum, D. P.; Linder, M.; Ernst, R. R. *J. Magn. Reson.* **1981**, *44*, 173–188.
(22) Bielecki, A.; Burum, D. P.; Rice, D, M.; Karasz, F. E. *Macromolecules* **1991**, *24*, 4820–4822.
(23) Simpson, J. H.; Ruggeri, G.; Rice, D. M.; Karasz, F. E. Submitted for publication.
(24) Stolka, M.; Yanus, J. F.; Pai, D. M. *J. Phys. Chem.* **1984**, *88*, 4707–4714.
(25) Pai, D. M.; Yanus, J. F.; Stolka, M. *J. Phys. Chem.* **1984**, *88*, 4714–4717.
(26) Prest, W. M. Unpublished data.
(27) Froix, M.; Goedde, A. O. Unpublished data.
(28) Dixon, W. T.; Schaefer, J.; Sefcik, M. D.; Stejskal, E. O.; McKay, R. A. *J. Magn. Reson.* **1982**, *49*, 341.
(29) Ziolo, R. F, Unpublished data.
(30) McBrierty, V. J. *Faraday Discuss. Chem. Soc.* **1979**, *68*, 1–9.
(31) Yuh, H.-J.; Pai, D. M. *Philos. Mag. Lett.* **1990**, *62*, 61–66.
(32) Hewitt, J. M.; Henrichs, P. M.; Scozzafava, M.; Scaringe, R. P.; Linder, M.; Sorriero, L. J. *Macromolecules* **1984**, *17*, 2566–2572.